RESEARCH ARTICLE

Macromolecular Chemistry and Physics
www.mcp-journal.de

Chemical Cascading Between Polymersomal Nanoreactor Populations

Yigit Altay, Antoni Llopis-Lorente, Loai K. E. A. Abdelmohsen, and Jan C.M. van Hest**

Special Issue dedicated to Brigitte Voit

Harnessing interactions of functional nano-compartments to generate larger particle assemblies allows studying diverse biological behaviors based on their population states and can lead to the development of smart materials. Herein, thiol-functionalized polymersome nanoreactors are utilized as responsive organelle-like nano-compartments—with inherent capacity to associate into larger aggregates in response to change in the redox state of their environment—to study the kinetics of cascade reactions and explore functions of their collective under different population states. Two nanoreactor populations, glucose oxidase- and horseradish peroxidase-loaded polymersomes, are prepared, and the results of their cascading upon addition of glucose are investigated. The kinetics of resorufin production in associated polymersomes and non-associated polymersome populations are compared, observing a decreased rate upon association. For the associated populations, faster chemical cascading is found when the two types of nanoreactors are associated in a concerted step, as compared to sequential association. The addition of competing agents such as catalase impacts the communication between non-associated polymersomes, whereas such an effect is less pronounced for the associated ones. Altogether, the results showcase the impact of collective associations on enzymatic cascading between organelle-like nanoreactors.

1. Introduction

Designing synthetic materials that can engage in some sort of biologically relevant behavior can lead to significant advancements, ranging from the development of advanced biosensing and catalysis nanotechnologies to providing insight into the underlying logic of biological life.[1,2] To translate life-like behaviors into synthetic materials, a variety of systems ranging from the molecular to the micron scale have been developed.[3,4] Functions of most of these designs, however, are often restricted to their individual state,[5–7] whereas their interaction and communication are so far underexplored.[8,9] In biology, however, functions are not just the result of the operation of single cells, but are mainly a consequence of their collective interaction.[10] Organizational operations, where supramolecular systems can reversibly switch between various structural and spatial states, are ubiquitous in controlling various biological processes, in which chemical information is translated into higher-order functions. For example, cytoskeletal proteins (e.g., actin, myosin), which are the structural sub-units of the cell cytoskeleton, assemble into filamentous microstructures that facilitate key processes such as movement, intracellular transport, signaling, proliferation, and apoptosis.[11] Proteins with higher number of subunits (i.e., secondary and tertiary) undergo directed assembly to adopt a specific surface topology (for assembly and recognition) and to display active sites (for catalysis and storage). In turn, recent advances in synthetic self-assembled structures based upon solid nano- (and micro-) particles showcase the potential to utilize chemical programming in the design of synthetic colloidal systems that can collectively interact, resulting in higher-order assemblies with emergent functions.[12–16] Examples include patchy colloids that can collectively interact via metal-coordination subunits.[17] Another example demonstrated DNA-guided association of colloidal nanoparticles.[18] Regardless of the chemistry used for such collective interaction, realizing pre-programmed synthetic nanostructures that can collectively interact, in response to an external trigger, and produce mesostructures with added functionalities, can facilitate the investigation of diverse biological processes. With this in mind, we are particularly interested in studying the changes

Y. Altay, A. Llopis-Lorente, L. K. E. A. Abdelmohsen, J. C. van Hest
Department of Chemical Engineering and Chemistry, Department of Biomedical Engineering, Institute of Complex Molecular Systems (ICMS)
Eindhoven University of Technology
Het Kranenveld 14, MB Eindhoven 5600, The Netherlands
E-mail: l.k.e.a.abdelmohsen@tue.nl; j.c.m.v.hest@tue.nl

A. Llopis-Lorente
Institute of Molecular Recognition and Technological Development (IDM), CIBER de Bioingeniería, Biomateriales y Nanomedicina (CIBER-BBN)
Universitat Politècnica de València
Camino de Vera s/n, Valencia 46022, Spain

The ORCID identification number(s) for the author(s) of this article can be found under https://doi.org/10.1002/macp.202200269

DOI: 10.1002/macp.202200269

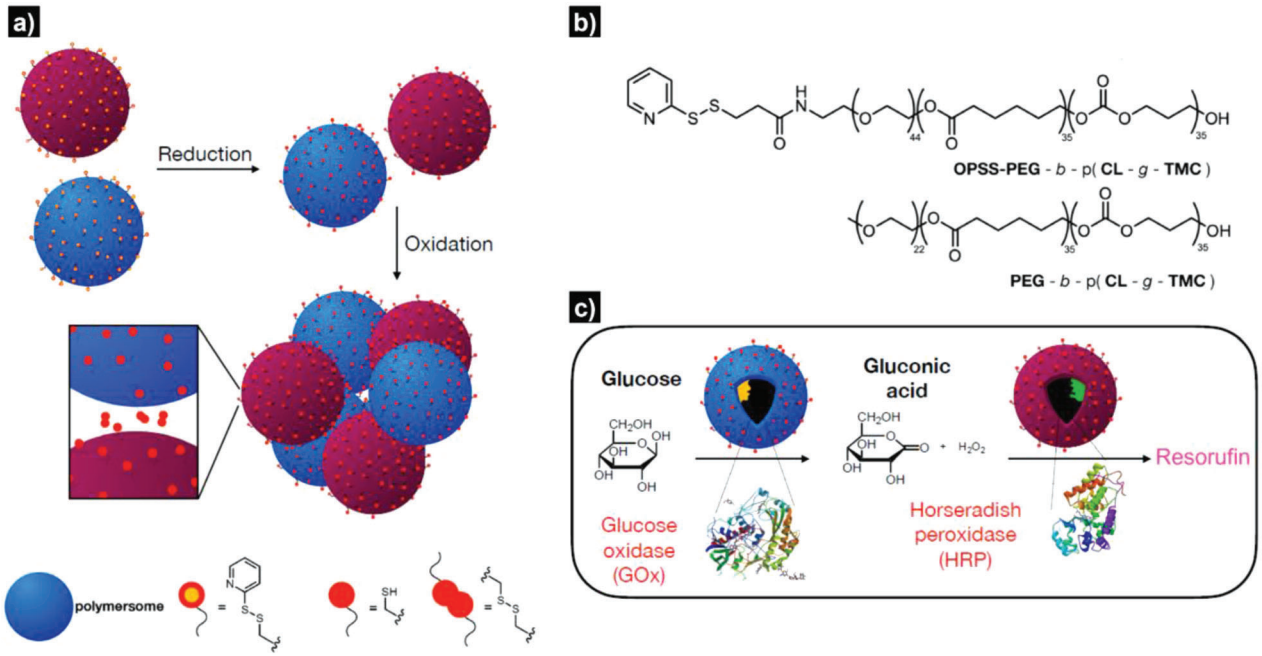

Figure 1. a) Schematic representation of the system. Thiols are deprotected by reduction to enable the thiol-disulfide exchange reaction between polymersomes. b) Chemical structures of the polymers used in this study. c) Schematic representation of the functional enzyme cascade that is GOx and HRP which are loaded into separate polymersome populations.

in the kinetics of chemical cascading upon the association of polymersomal nanoreactors into higher-order aggregates.

Among different types of synthetic particles, polymersomes are soft colloids that offer an optimal framework for engineering and investigating changes in embedded biological processes upon their collective association. Such copolymeric vesicles are capable of encapsulating active catalysts in their aqueous lumen or hydrophobic membrane, and are also referred to as artificial nano-organelles.[19–21] Polymersomal particles possess a high degree of structural and functional versatility due to the ability to nanoengineer their structural characteristics through chemical and physical means.[22,23] Recently, our group demonstrated thiol-functionalized micellar structures that were capable of engaging in dynamic and transient interactions, switching between associated and non-associated states, via oxidation and reduction cycles.[24] Capitalizing on this, we herein leverage the ability of engineered polymersome nanoreactors to collectively associate, allowing the investigation of chemical cascading between complementary compartmentalized enzymes. In particular, we employ a unique platform based on semi-permeable, poly(ethylene glycol)-block-poly(caprolactone-gradient-trimethylene carbonate) (PEG-P(CLgTMC)) polymersomes, incorporating a thiol functionality at the PEG chain end. These compartments can be loaded with enzymes, and substrates and products can freely diffuse in and out.[25] They are furthermore mechanically stable and chemically versatile. Due to their unique features, these polymersomes are excellent candidates for the development of systems, which are not only able to undergo collective assembly into larger structures, but also impart a higher degree of functionality to control such process. In our approach, polymersome association is induced by the addition of reducing and oxidizing agents (**Figure 1**), via deprotection of the thiol groups (by the reducing agent) at the PEG end (Figure 1a,b) and subsequent formation of disulfide bridges between particles. This allows us to investigate chemical cascading between two polymersome populations containing complementary enzymes, that is, the cascade reaction between glucose oxidase (GOx) and horseradish peroxidase (HRP) as a model system, which results in the conversion of Amplex Red to resorufin as a fluorescent product (Figure 1c). Using this unique platform, here we set out to investigate chemical cascading in i) non-associated and associated polymersome populations, ii) nanoreactors associated in a sequential or concerted process, and iii) the influence of competing agents in the media; thus, providing valuable insights into the performance of enzymatic cascading between organelle-like nanoreactors.

2. Results and Discussion

For the development of the nanoreactors, polymersomes were prepared from the amphiphilic block copolymer poly(ethylene glycol)-block-poly(caprolactone-gradient-trimethylene carbonate) (PEG_{22}-*b*-P(CL_{35}-*g*-TMC_{35})), using our previously reported direct hydration procedure.[25,26] To endow the polymersomes with reversible association capability, a copolymer comprising a thiol functionality at the PEG chain end was added (10 wt.%) during polymersome formation (Figure 1b). This polymer was synthesized by ring-opening polymerization of caprolactone and trimethylene carbonate, with ortho-pyridyldisulfide (OPSS) functionalized PEG as a macroinitiator. In order to facilitate thiol-disulfide exchange, a longer PEG chain was used for the thiol-functional building block (OPSS-PEG_{44}-*b*-P(CL_{35}-*g*-TMC_{35})). The ortho-pyridyl thiol (OPS) functionality acted as a protecting group and prevented interaction between the formed polymersomes prior to the addition of redox reagents. The length

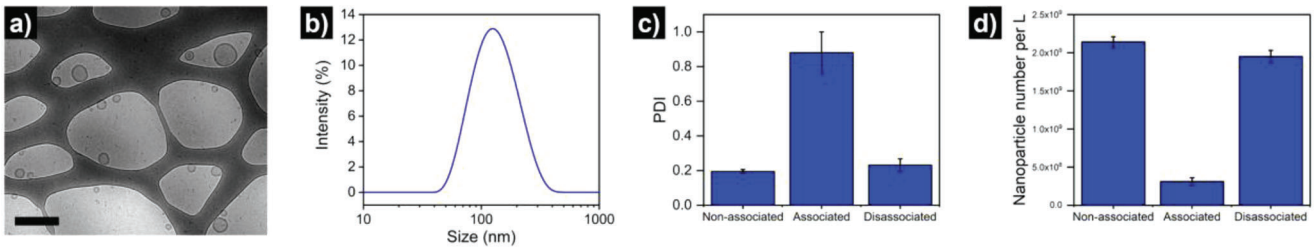

Figure 2. a) Cryo-TEM image of thiol-functionalized polymersomes. Scale bar = 500 nm. b) Hydrodynamic diameter intensity distribution of thiol-functionalized polymersomes, as measured by DLS. Average size = 123 ± 1 nm, PDI = 0.194 ± 0.012). c) PDI of the polymersomes (non-associated), associated polymersomes after addition of sodium perborate tetrahydrate (associated), and disassociated polymersomes after addition of TCEP (disassociated), as measured by DLS. d) Particle count of the polymersomes (non-associated), associated polymersomes after addition of sodium perborate tetrahydrate (associated), and disassociated polymersomes after addition of TCEP (disassociated), as measured by DLS. Please note the drop in particle count and its restoration upon association and disassociation.

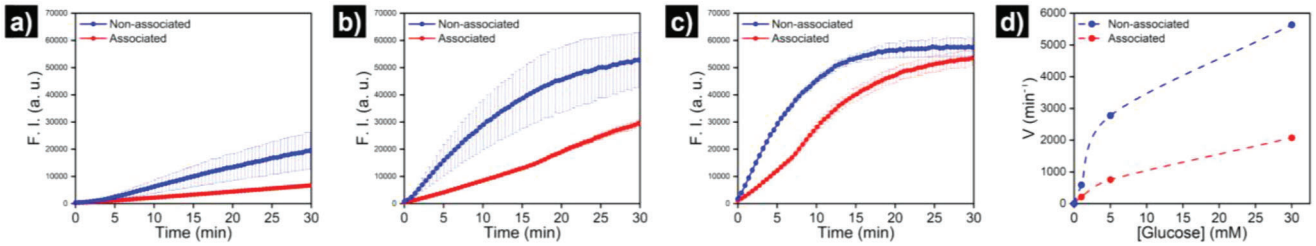

Figure 3. Fluorescence intensity corresponding to resorufin production over time at a) 1, b) 5, and c) 30 mM glucose concentration using non-associated and associated nanoreactor samples. Results are represented as mean ± s.d. (n = 3). d) Extracted velocities from the slope of the plots.

and Đ of both polymers were characterized using ^{1}H NMR (Figures S1 and S2, Supporting Information) and gel permeation chromatography (GPC), respectively. (PEG_{22}-*b*-P(CL_{35}-*g*-TMC_{35}) and (OPSS-PEG_{44}- *b*-P(CL_{35}-*g*-TMC_{35}) had a Đ of 1.17 and 1.19, respectively. The morphological integrity of the polymersomes was confirmed using cryo-genic electron microscopy (cryo-TEM) (**Figure 2**a) and dynamic light scattering (DLS) (Figure 2b). The polymersomes had an average hydrodynamic size of 123 nm and a polydispersity index (PDI) of ca. 0.2. Utilizing reversible disulfide chemistry, polymersome collective association was induced by sequential addition of reducing and oxidizing agents; namely, tris(2-carboxyethyl)phosphine) hydrochloride (TCEP, 0.8 mM, to induce the deprotection of thiol groups) and sodium perborate tetrahydrate (0.8 mM, to induce the formation of disulfide bridges, see Supporting Information for details). The mixture was incubated for 20 min under magnetic stirring at 300 rpm to allow polymersome association. Upon polymersome association, a significant increase in PDI (Figure 2c) and a decrease in nanoparticle count (by nanoparticle tracking analysis (NTA)) were observed (Figure 2d), as a consequence of the formation of large aggregates (estimated size 2–5 μm, Figure S3, Supporting Information). The high PDI values (>0.8) upon association indicated high polydispersity of the aggregates—aggregates with finely controlled size (i.e., low polydispersity) could not be obtained under our experimental conditions. Particle count and DLS size distribution were restored upon the addition of additional TCEP and consequent aggregate disassociation (measured after 20 min incubation upon stirring at 300 rpm), in agreement with our previous study.[24] Such reversible association and disassociation processes did not impact the polymersome's morphological integrity, evident from DLS data and cryo-TEM images (Figures S4 and S5, Supporting Information).

After validating the assembly behavior of the polymersomes, we set out to evaluate how the state of association affected chemical cascading between polymersomal nanoreactors with encapsulated enzymes. To provide the polymersomes with biocatalytic activity the enzymes GOx and HRP were directly incorporated during the assembly process at a concentration of 5 mg mL^{-1}. Non-encapsulated proteins were removed using size exclusion chromatography (SEC), and enzyme encapsulation was confirmed by the Bradford assay. Encapsulation efficiency was calculated to be 7.4% and 8.3%, for GOx and HRP, respectively; which corresponds to 18.5 μg of GOx and 20.8 μg of HRP per mg of polymer. Enzyme encapsulation did not have a significant impact on the DLS intensity profile and PDI of the particles (Figures S6 and S7, Supporting Information). As a model system, we employed the well-known cascade reaction, in which GOx oxidizes glucose, forming hydrogen peroxide (H_2O_2), which is used by the second enzyme, HRP to convert Amplex Red into the fluorescent compound resorufin. We compared the activity of associated versus non-associated polymersomes (5 mg mL^{-1}) at various glucose concentrations (0, 1, 5, and 30 mM). No conversion was observed in the absence of glucose (Figure S8, Supporting Information), which confirmed its key role to trigger communication. In presence of glucose, at all concentrations, a clear increase in fluorescence resulting from resorufin production was observed for both associated and non-associated polymersomes. Higher glucose concentration led to faster kinetics for both associated and non-associated polymersomes, yet we observed significantly faster conversion for non-associated populations at all glucose concentrations (**Figure 3**a–d). The

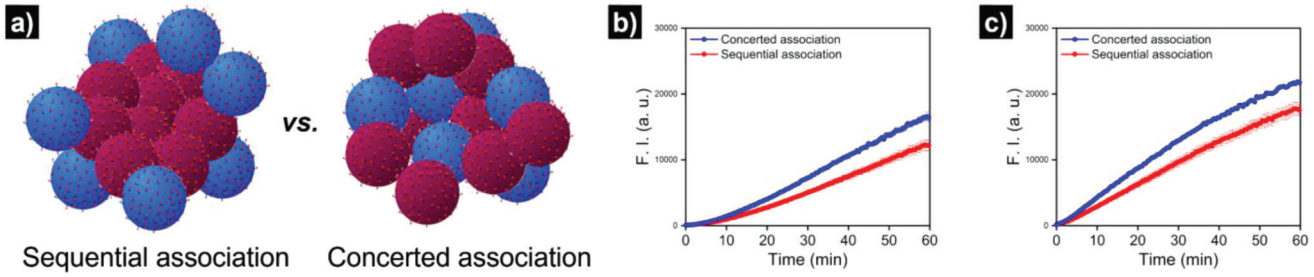

Figure 4. a) Schematic representation of sequential versus concerted association of polymersomes. Fluorescence intensity corresponding to resorufin production over time at b) 1 and c) 5 mM of glucose. Results are represented as mean ± s.d. (n = 3).

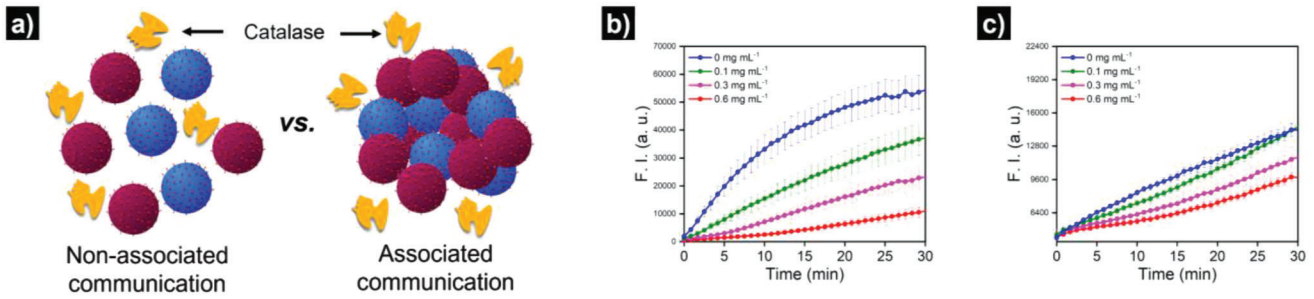

Figure 5. a) Schematic representation of the catalase competition in the GOx-HRP cascade system comparing non-associated versus associated polymersomes. Fluorescence intensity corresponding to resorufin production over time at various catalase concentrations (0 to 0.6 mg mL^{-1}) for b) non-associated and c) associated polymersomes. Results are represented as mean ± s.d. (n = 3).

resulting reaction velocities were extracted from the slope of the plots by linear fitting over the first 5 min. Non-associated polymersomes displayed reaction velocities between 2.2 to 4 times higher than associated polymersomes. As an explanation for the faster kinetics of non-associated polymersomes, we hypothesized that the assembly of the nanoreactors leads to an additional diffusion barrier for the dissolved glucose to penetrate into the nanoreactors that are in the core of the associated polymersomes. Thus, non-associated polymersomes—with higher diffusivity and more exposed surface—have better access to glucose present in the media to initiate the communication cascade and result in faster product formation.

In the next step, we evaluated the impact of nanoreactors' spatial location on the enzymatic cascade, by associating the two communicating populations in either a sequential or a concerted fashion (**Figure 4**a). In a concerted fashion, GOx- and HRP-nanoreactors were simultaneously associated and thus located in near proximity to each other in mixed aggregates. In the sequential oxidation, HRP nanoreactors (depicted in red in Figure 4a) were first associated and in a second step, GOx-nanoreactors were added and let to associate on the clusters of HRP-containing polymersomes—thus, resulting in HRP-nanoreactors in the core of the aggregate and locating GOx-nanoreactors on the surface. Again, no signal was observed upon the addition of Amplex Red in the absence of glucose (Figure S9, Supporting Information). We then monitored resorufin production in the presence of glucose at 1 and 5 mM concentrations for both sequentially and concertedly associated polymersomes. Interestingly, the concertedly associated nanoreactors exhibited an increase in the rate of resorufin production of ca. 35% (at both glucose concentrations tested) compared to their sequentially associated counterparts (Figure 4b,c, Figure S10, Supporting Information)—this observation could be ascribed to the faster exchange of H_2O_2 (as chemical messenger between the communicating polymersomes), when they are located in increased proximity to each other within the aggregates.

In a final step, we investigated the effect of introducing a competing agent that would consume the chemical messenger exchanged between the two polymersome populations. In particular, we added catalase to the reaction medium—as it is an active enzyme that consumes H_2O_2 and could thus interfere in the communication between GOx and HRP nanoreactors (see schematic in Figure S11, Supporting Information, and **Figure 5**a). In these experiments, we evaluated the effect of such competing agent in non-associated and associated polymersome populations using different catalase concentrations in the environment (0, 0.1, 0.3, and 0.6 mg mL^{-1}). Glucose was added at 30 mM and then resorufin production was monitored over time. Interestingly, the resorufin production decay in the presence of catalase was much more pronounced for the non-associated polymersomes (Figure 5b,c and Figure S12, Supporting Information) reaching an 85% reduction in activity with 0.6 mg mL^{-1} of catalase. In both cases, higher catalase concentrations led to a larger activity decay, yet the effect was less pronounced for associated polymersomes. These observations may suggest that in the associated polymersomes the exchanged chemical messenger (H_2O_2) is mainly transmitted to neighbor nanoreactors within the aggregate; thus, the presence of free catalase in the external environment does not have a large effect on the chemical cascading. This effect (resistance to catalase competition) is expected to be

reduced when reducing the aggregate size, yet control over aggregate size was not achieved under our experimental conditions—achieving a fine control over the aggregate size and studying chemical cascading in such nanoreactor assemblies as a function of their size is an interesting prospect for future studies.

3. Conclusion

In summary, we designed thiol-functionalized semipermeable polymersomes that are able to reversibly and collectively associate (aggregate) and disassociate, depending on the redox state. We studied the impact of polymersomes' aggregation state on chemical cascading between two communicating nanoreactor populations. When the nanoreactors were in the associated state, a decrease in the rate of product formation was observed compared to non-associated nanoreactors. We attributed such a drop in chemical cascading to an additional diffusional barrier for the nanoreactors located in the core of the aggregates. Thereafter, we evaluated the effect of the nanoreactors' spatial location within the aggregate, by comparing the effect of sequential (i.e., GOx-nanoreactors associated on the surface of HRP-nanoreactor clusters) and concerted association of nanoreactors in the chemical cascading process. Product formation was faster when the two nanoreactor populations were simultaneously associated in a concerted process, due to the spatial proximity of communicating nanoreactors. Finally, we evaluated the effect of the presence of a competing agent in the communication between polymersomes, observing a large decay in the product formation rate for non-associated polymersomes. This effect was less pronounced for associated polymersomes which suggests that they mainly exchange chemicals within the aggregate and are less affected by the presence of competing agents in the solution. Altogether, we believe our study offers valuable insights into the impact of nanoreactors' association in chemical cascading and may inspire further advances in the fields of interactive materials, biomimicry, and artificial cell research.

Supporting Information

Supporting Information is available from the Wiley Online Library or from the author.

Acknowledgements

Y.A. and A.L.-L. contributed equally to this work. The authors would like to acknowledge the support from the Dutch Ministry of Education, Culture, and Science (Gravitation program 024.001.035 and Spinoza premium) and the ERC Advanced Grant (Artisym 694120).A.L.-L. acknowledges support from the MSCA Cofund project oLife, which has received funding from the European Union's Horizon 2020 research and innovation program under the Grant Agreement 847675; and the María Zambrano Program from the Spanish Government funded by NextGenerationEU from the European Union. Dr. Imke Pijpers is thanked for cryo-TEM imaging. Dr. Pascal Welzen is acknowledged for advice and useful discussion on polymer and polymersome preparation.

Conflict of Interest

The authors declare no conflict of interest.

Data Availability Statement

The data that support the findings of this study are available from the corresponding author upon reasonable request.

Keywords

chemical cascading, enzymes, nanoparticles, nanoreactors, polymersomes

Received: July 28, 2022
Revised: August 18, 2022
Published online: September 9, 2022

[1] R. Merindol, A. Walther, *Chem. Soc. Rev.* **2017**, *46*, 5588.
[2] S. A. P. Van Rossum, M. Tena-Solsona, J. H. Van Esch, R. Eelkema, J. Boekhoven, *Chem. Soc. Rev.* **2017**, *46*, 5519.
[3] H. W. H. Van Roekel, B. J. H. M. Rosier, L. H. H. Meijer, P. A. J. Hilbers, A. J. Markvoort, W. T. S. Huck, T. F. A. De Greef, *Chem. Soc. Rev.* **2015**, *44*, 7465.
[4] M. Nijemeisland, L. K. E. A. Abdelmohsen, W. T. S. Huck, D. A. Wilson, J. C. M. Van Hest, *ACS Cent. Sci.* **2016**, *2*, 843.
[5] L. Schoonen, J. C. M. Van Hest, *Adv. Mater.* **2016**, *28*, 1109.
[6] E. Rideau, R. Dimova, P. Schwille, F. R. Wurm, K. Landfester, *Chem. Soc. Rev.* **2018**, *47*, 8572.
[7] B. C. Buddingh', J. C. M. Van Hest, *Acc. Chem. Res.* **2017**, *50*, 769.
[8] B. De Luis, A. Llopis-Lorente, F. Sancenón, R. Martínez-Máñez, *Chem. Soc. Rev.* **2021**, *50*, 8829.
[9] B. De Luis, Á. Morellá-Aucejo, A. Llopis-Lorente, T. M. Godoy-Reyes, R. Villalonga, E. Aznar, F. Sancenón, R. Martínez-Máñez, *Chem. Sci.* **2021**, *12*, 1551.
[10] N. Yeh Martín, L. Valer, S. S. Mansy, *Emerging Top. Life Sci.* **2019**, *3*, ETLS20190026.
[11] G. Pawlak, D. M. Helfman, *Curr. Opin. Genet. Dev.* **2001**, *11*, 41.
[12] M. Grünwald, P. L. Geissler, *ACS Nano* **2014**, *8*, 5891.
[13] N. Vogel, S. Utech, G. T. England, T. Shirman, K. R. Phillips, N. Koay, I. B. Burgess, M. Kolle, D. A. Weitz, J. Aizenberg, *Proc. Natl. Acad. Sci. USA* **2015**, *112*, 10845.
[14] J. Li, D. K. Baxani, W. D. Jamieson, W. Xu, V. G. Rocha, D. A. Barrow, O. K. Castell, *Adv. Sci.* **2020**, *7*, 1901719.
[15] A. Altemose, M. A. Sánchez-Farrán, W. Duan, S. Schulz, A. Borhan, V. H. Crespi, A. Sen, *Angew. Chem., Int. Ed.* **2017**, *56*, 7817.
[16] L. Rodríguez-Arco, B. V. V. S. P. Kumar, M. Li, A. J. Patil, S. Mann, *Angew. Chem., Int. Ed.* **2019**, *58*, 6333.
[17] Y. Wang, A. D. Hollingsworth, S. K. Yang, S. Patel, D. J. Pine, M. Weck, *J. Am. Chem. Soc.* **2013**, *135*, 14064.
[18] D. Nykypanchuk, M. M. Maye, D. Van Der Lelie, O. Gang, *Nature* **2008**, *451*, 549.
[19] R. J. R. W. Peters, I. Louzao, J. C. M. Van Hest, *Chem. Sci.* **2012**, *3*, 335.
[20] J. Gaitzsch, X. Huang, B. Voit, *Chem. Rev.* **2016**, *116*, 1053.
[21] S. F. M. Van Dongen, W. P. R. Verdurmen, R. J. R. W. Peters, R. J. M. Nolte, R. Brock, J. C. M. Van Hest, *Angew. Chem., Int. Ed.* **2010**, *49*, 7213.
[22] D. E. Discher, A. Eisenberg, *Science* **2002**, *297*, 967.
[23] D. E. Discher, F. Ahmed, *Annu. Rev. Biomed. Eng.* **2006**, *8*, 323.
[24] Y. Altay, I. A. B. Pijpers, L. K. E. A. Abdelmohsen, J. C. M. Hest, *ChemSystemsChem* **2019**, *1900049*, 2.
[25] L. M. P. E. Van Oppen, L. K. E. A. Abdelmohsen, S. E. Van Emst-De Vries, P. L. W. Welzen, D. A. Wilson, J. A. M. Smeitink, W. J. H. Koopman, R. Brock, P. H. G. M. Willems, D. S. Williams, J. C. M. Van Hest, *ACS Cent. Sci.* **2018**, *4*, 917.
[26] P. L. W. Welzen, S. W. Martinez Ciriano, S. Cao, A. F. Mason, I. A. B. Welzen-Pijpers, J. C. M. Hest, *J. Polym. Sci.* **2021**, *59*, 1241.